

Texture Analysis of Damascene Copper Interconnects*

Wang Xiaodong^{1,†}, Ji Yuan², Zhong Taoxing², Li Zhiguo³, Xia Yang⁴,
Liu Danmin², and Xiao Weiqiang²

(1 Basic Department, Chinese People's Armed Police Forces Academy, Langfang 065000, China)

(2 Institute of Microstructure and Property of Advanced Materials, Beijing University of Technology, Beijing 100022, China)

(3 School of Electronic Information & Control Engineering, Beijing University of Technology, Beijing 100022, China)

(4 Microelectronics R & D Center, Chinese Academy of Sciences, Beijing 100029, China)

Abstract: Texture and grain boundary character distribution of Cu interconnects with different line width for as-deposited and annealed conditions were measured by EBSD. All specimens appear mixed texture and (111) texture is the dominate component. As-deposited interconnects undergo the phenomenon of self-annealing at RT, in which some abnormally large grains are found. Lower aspect ratio of lines and anneal treatment procured larger grains and stronger (111) texture. Meanwhile, the intensity proportion of other textures with lower strain energy to (111) texture is decreased. As-deposited specimens reveal (111)<112> and (111)<231> components. (111)<110> component appeared and (111)<112> and (111)<231> components were developed during the annealing process. High angle boundaries are dominant in all specimens, boundaries with a misorientation of 55°~60° and $\Sigma 3$ ones in higher proportion, followed by lower boundaries with a misorientation of 35°~40° and $\Sigma 9$ boundaries. As the aspect ratio of lines and anneal treatment increase, there is a gradual increment in $\Sigma 3$ boundaries and a decrease in $\Sigma 9$ boundaries.

Key words: Cu interconnects; texture; misorientation; coincident site lattice boundaries; EBSD

EEACC: 0290T

CLC number: TN406

Document code: A

Article ID: 0253-4177(2008)06-1136-05

1 Introduction

With the development of faster and smaller integrated circuits, the replacement of Al by Cu has been a tendency in interconnects technology. Microstructure is the key factor that determines the reliability of metal films and interconnects. Al interconnects with large grains and (111) fiber texture were shown to have better EM (electromigration) resistance. Recently, the impact of grain structure and texture on electromigration (EM) and stress that induced failures in Cu interconnects has been reported. Because of Damascene inlaid structure in Cu interconnects, the texture evolution is a function of line width, aspect ratio of depth to width, anneal treatment, and stress state, etc. It is difficult to identify precisely the reasons for texture formation and evolution, which leads to different reported textures in Cu interconnects by different authors^[1~4]. In this paper, we present the texture and grain boundary character distribution analysis of both as-deposited and annealed Cu interconnects with different line width.

2 Experiment

Three different Damascene Cu interconnects were investigated using electron backscattered diffraction (EBSD). The line width/pitch distances of 4 μm and 2 μm lines were 0.125/4 and 0.25/2, respectively, and the depth of the trenches was 0.5 μm . A 50nm thick Ta layer and a 50nm layer of Cu seed were successively deposited on the trench by magnetron sputtering, subsequently filing the trench by electroplating with Cu, and finally removing excess Cu by chemical mechanical polishing. Parts of the 2 μm specimens were annealed at 300°C for 30min in N₂ gas to avoid oxide formation on the top of Cu interconnects. An EDAX-EBSD system mounted on a Philips XL-30 SEM measured (111), (100), and (110) pole figures, and orientation distribution functions (ODF) were calculated using the series expansion method of Bunge-system^[5]. At the same time, the distribution of grain size, grain boundary misorientation, and coincident site lattice (CSL) boundaries were measured. The EBSD data were collected over an area of 32 μm × 184 μm

* Project supported by the National Natural Science Foundation of China (No.69936020)

† Corresponding author. Email: wwxiaodong@yahoo.com.cn

Received 29 October 2007, revised manuscript received 17 February 2008

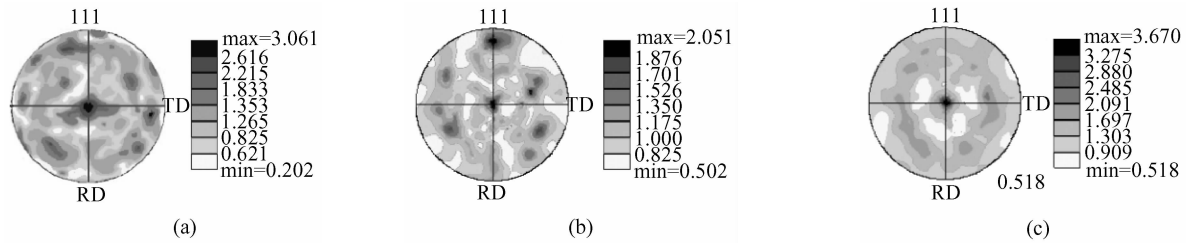


Fig. 1 Normalized (111) pole figures for as-deposited $4\mu\text{m}$ (a), as-deposited $2\mu\text{m}$ (b), and annealed $2\mu\text{m}$ (c) Cu interconnects

Table 1 Intensity ratio of other textures components to (111) component in (111) pole figures of Cu interconnects

Specimen	(111)	(100)	(511)	(310)	(311)	(210)	(320)	(211)	(321)	(331)	(221)
As-deposited $4\mu\text{m}$ lines	1	59.9	–	59.9	59.9	72.4	44.2	59.9	41.2	–	–
As-deposited $2\mu\text{m}$ lines	1	77.4	91.5	57.2	1	65.8	–	74.4	82.8	48.7	57.2
Annealed $2\mu\text{m}$ lines	1	57.0	–	46.2	46.2	46.2	–	57.0	–	–	–

with $0.10\mu\text{m}$ step size for as-deposited $4\mu\text{m}$ lines, $28\mu\text{m} \times 88\mu\text{m}$ with $0.07\mu\text{m}$ step size for as-deposited $2\mu\text{m}$ lines, and $36\mu\text{m} \times 196\mu\text{m}$ with $0.10\mu\text{m}$ step size for annealed $2\mu\text{m}$ lines, respectively.

3 Results and discussion

Figure 1 shows the (111) pole figures for three different Cu interconnects. All specimens reveal mixed texture. Intensity ratio of other textures components to (111) component in (111) pole figures of Cu lines are contained in Table 1. The strain energy of (100) to (221) grain planes, which appear from left to right in Table 1, increase by degrees^[6]. The results indicate that (111) texture is the dominate component slightly. The intensity of (100), (511), (310), and (311) texture components with lower stain energy approach the (111) component's in as-deposited $2\mu\text{m}$ lines. However, the intensity ratio of textures with grain planes with lower strain energy to (111) texture decreases with increasing line width and annealing process. The important effect on the evolution of texture during deposition and annealing procedure is from minimization of anisotropic surface energy of films, interface energy between the film and substrate, and strain energy. The close-packed (111) planes have the lowest surface/interface energy, so the surface/interface energy of system is at minimum with a (111) texture. (111) orientation grains can be merged by grains having lower strain energy at the process of minimum of films stain energy due to its highest strain energy^[7]. We can presume that surface/interface energy plays a major role in evolution of texture, followed by strain energy. Anneal treatment can strengthen the dominate level of the surface/interface energy. As the aspect ratio increases, the effect of strain energy on the evolution of texture becomes sharper.

Curves of area fraction verse grain size were measured by EBSD, as shown in Fig. 2. The curves corresponding to annealed specimens exhibit single-peaked behavior. However, that of the as-deposited lines exhibit bimodal behavior. The grain sizes of the as-deposited $4\mu\text{m}$ and $2\mu\text{m}$ lines are $2.8\mu\text{m}$ and $2.4\mu\text{m}$, respectively. The large grain size at the second peak and its lower proportion of area indicate the presence of several abnormally large grains in lines. These grains growth speed is decided by two factors: first, the driving force of grain boundaries migration, which depends upon D-values of the density of surface/interface energy and strain energy, the decreasing of normal grains grain boundaries area, and the increment of abnormal grains grain boundaries area, and, second, grain boundaries activity corresponding to diffusion activation energy^[8]. As the orientation of abnormal grains make the sum of the films surface/interface energy and strain energy minimal, the growing speed is by zero and the structure is non-active. We can not test the orientation of abnormal grains. Additional studies are required. In addition, compared with as-deposited $2\mu\text{m}$ lines, the grain size distribution for the other two specimens indicates lower aspect ratio of lines with larger grains and growing of grains by anneal treatment, which is shifted to the right.

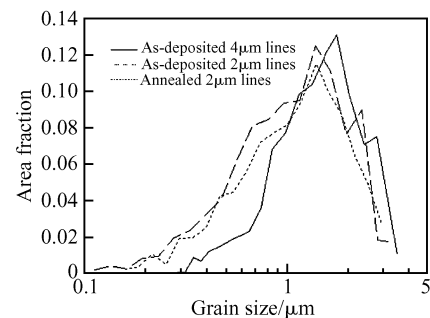


Fig. 2 Curves of area fraction versus grain size of Cu interconnects

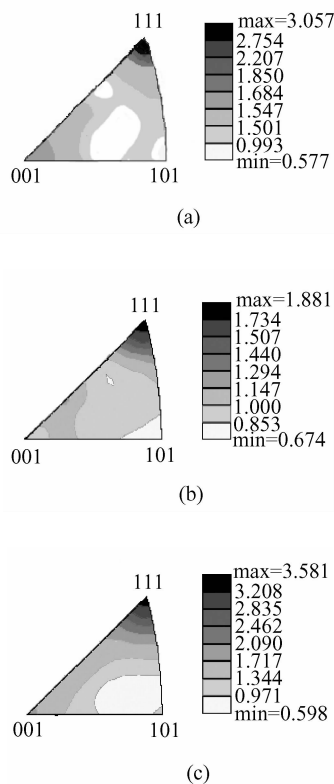


Fig.3 Normalized (111) inverse pole figures for as-deposited $4\mu\text{m}$ (a), as-deposited $2\mu\text{m}$ (b), and annealed $2\mu\text{m}$ (c) Cu interconnects

Figure 3 shows normalized (111) inverse pole figures. That the gradual weakening of (111) texture intensity with the narrowing of line width appearing in as-deposited interconnects is attributed to nucleation competitions between the side-wall and bottom of the trenches^[9]. Observation of reduced (111) texture of 1 to $4\mu\text{m}$ annealed Cu lines with a 50nm Ta barrier layer has been reported by Mirpuri *et al.*^[10], but an opposite phenomenon is observed in our experiments. Considering similar line width and aspect ratio, the variant thermal stress states provoked by different pitch distance of Cu interconnects is one possibility that can induce variant evolution of the texture, which is generated during the annealing process. A

weak (110) texture exists in annealed specimens (Fig. 3(c)). The lowest index plane perpendicular to (111) is (110). It is assumed that a (110) texture parallel to the surface of interconnects appears for (111) texture with $\langle 111 \rangle$ direction perpendicular to the side-wall of trenches^[7]. Anneal treatment intensified (111) texture parallel to the side-wall and bottom synchronously. As a result of less nucleation area of sidewall in contrast to the bottom, annealed specimens have a weak (110) texture.

To analyze the changes of (111) texture components in as-deposited and annealed Cu interconnects with different line width, ODFs were calculated. Sections of ODFs for $\phi_2 = 45^\circ$ are shown in Fig. 4. (111) and (115) texture intensity of Cu lines are presented in Table 2. Having low fault energy, copper can generate annealing twin. Twinning of (111) planes produced (115) texture upon annealing^[11]. The (115) $\langle \bar{1}40 \rangle$ components appear in annealed specimens and (115) $\langle 1\bar{1}0 \rangle$ appear in as-deposited specimens from Table 2, which indicate the specimens undergo self-annealing at RT. (111) $\langle 112 \rangle$ and (111) $\langle 231 \rangle$ components appeared in as-deposited lines. Because Young's modulus is minimized in the $\langle 100 \rangle$ direction for FCC metals, grains whose $\langle 100 \rangle$ parallel to absolute maximum stress direction will grow precedence over other grains. The $\langle 112 \rangle$ and $\langle 231 \rangle$ directions, which are normal to the (111) direction and parallel to the plane consisting of the $\langle 111 \rangle$ direction, and the maximum stress direction have smaller angles with $\langle 100 \rangle$ directions. However, the $\langle 100 \rangle$ direction is not on the (111) plane. Therefore, (111) $\langle 112 \rangle$ or (111) $\langle 231 \rangle$ texture components will develop preferentially to others^[12]. Constraints of the sidewall of trenches may cause high strain states so that the growing of (111) $\langle 112 \rangle$ and (111) $\langle 231 \rangle$ components were made by minimum of stress during the self-annealing process. We infer that further minimum of stress strengthened (111) $\langle 112 \rangle$ and (111) $\langle 231 \rangle$ components in annealed specimens.

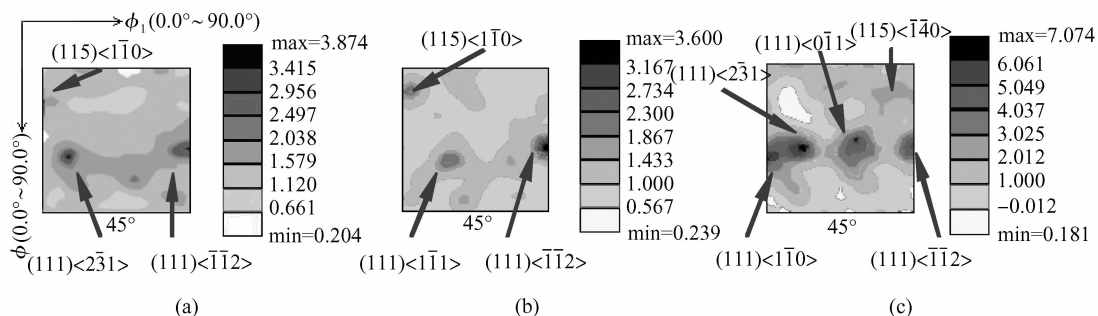


Fig.4 Sections of ODFs for $\phi_2 = 45^\circ$ as-deposited $4\mu\text{m}$ (a), as-deposited $2\mu\text{m}$ (b), and annealed $2\mu\text{m}$ (c) Cu interconnects

Table 2 (111) and (511) texture intensity of Cu interconnects

Specimen	(111) $\langle 1\bar{1}0 \rangle$	(111) $\langle 0\bar{1}1 \rangle$	(111) $\langle \bar{1}\bar{1}2 \rangle$	(111) $\langle 2\bar{3}1 \rangle$	(111) $\langle 1\bar{1}1 \rangle$	(115) $\langle 1\bar{1}0 \rangle$	(115) $\langle \bar{1}40 \rangle$
As-deposited 4 μm lines	–	–	3.874	3.874	–	1.579	–
As-deposited 2 μm lines	–	–	3.600	–	1.867	2.300	–
Annealed 2 μm lines	5.049	6.061	5.049	7.074	–	–	3.025

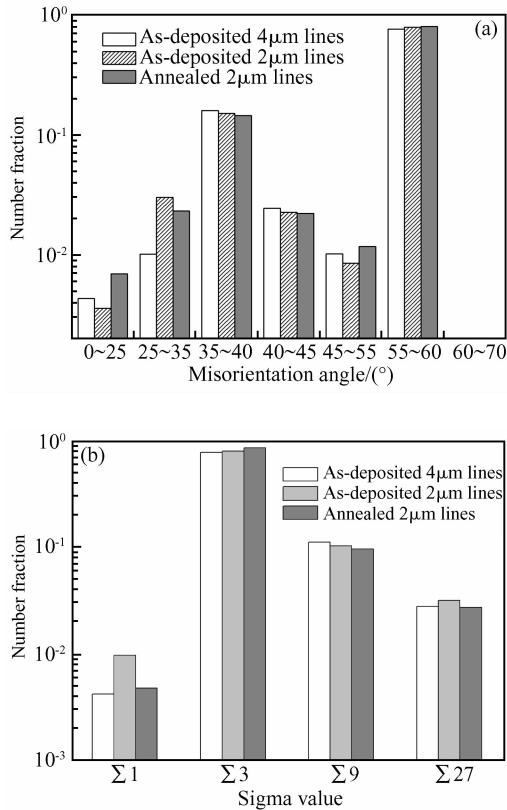


Fig. 5 Grain boundaries misorientation distribution (a) and CSL boundaries distribution (b) of Cu interconnects

Figure 4 shows that (111) $\langle 110 \rangle$ components are present upon annealing. Lee *et al.* argue that the stress state forms (111) $\langle 110 \rangle$ components^[12]. After the annealing process, Ta wires can appear at a higher intensity of (111) $\langle 110 \rangle$ components reported by some authors^[13]. Through an epitaxial effect, annealed texture of Ta barrier layer might play another significant role for the growing of (111) $\langle 110 \rangle$ components. At this point, additional studies are required to clarify this finding.

Figures 5 (a) and (b) show the grain boundaries misorientation distribution and the CSL boundaries distribution of three specimens, respectively. Above 70% $\Sigma 3$ boundaries in Cu interconnects indicates the presence of many twins. Therefore, lower texture intensity of specimens was observed before. High angle

Table 3 Proportions of low energy CSL boundaries ($\Sigma 3$) to high energy CSL boundaries ($\Sigma 9, \Sigma 27$)

Specimen	Proportion
As-deposited 2 μm lines	5.97
Annealed 2 μm lines	7.01

boundaries are dominant in all specimens, among which, there is a highest fraction of boundaries with a misorientation of $55^\circ \sim 60^\circ$ and $\Sigma 3$ boundaries, followed by boundaries with a misorientation of $35^\circ \sim 40^\circ$ and $\Sigma 9$ boundaries. As the aspect ratio and anneal treatment increase, there is a gradual increment in the misorientation of $55^\circ \sim 60^\circ$ and $\Sigma 3$ boundaries, and a decreasing in the misorientation of $35^\circ \sim 40^\circ$ and $\Sigma 9$ boundaries. Because of lower fault energy in copper, Cu films are liable to generate twin boundaries ($\Sigma 3$ boundaries) with low energy and at the same time inhibit the appearance of a dislocation slide during the deposition and recrystallization process^[14,15]. The possible reason that the fraction of $\Sigma 3$ boundaries is higher in as-deposited 2 μm lines than in 4 μm lines is from the formation of large twins in as-deposited 2 μm lines according to the higher level of self-annealing treatment because of minimization of system energy. We can observe much lower energy grain boundaries and a reduced proportion of high energy grain boundaries in specimens at 300 $^\circ\text{C}$ for 30min from Fig. 5 and Table 3. It is inferred that $\Sigma 9$ boundaries and others whose energy is relatively high migrated selectively to translate into $\Sigma 3$ twin boundaries and the reliability of EM resistance is improved effectively.

4 Conclusion

Texture and grain boundary distribution of Cu interconnects with different linewidth in as-deposited and upon annealing conditions were measured by EBSD. The driving force of evolution of texture and the growth and recrystallization of grains are attributed to the minimization of surface/interface and strain energy. For dominance of surface/interface energy, the intensity of (111) texture is highest in all specimens. The dominance is enhanced upon annealing. The effect of strain energy on the evolution of texture becomes sharper with the gradual decrease of line width. Higher aspect ratios of lines have smaller grains and weaker (111) texture for the effect of nucleation of sidewall. (111) $\langle 112 \rangle$ and (111) $\langle 231 \rangle$ components appeared in as-deposited specimens and developed upon annealing. Annealed texture of Ta barrier layer may work on the growing of the (111) $\langle 110 \rangle$ component. Boundaries with misorientation of $55^\circ \sim 60^\circ$ and $\Sigma 3$ boundaries have the highest fraction in Cu

interconnects. An increment with $\Sigma 3$ boundaries and a decrease with $\Sigma 9$ boundaries etc. in annealed specimens indicate that high energy boundaries migrated selectively.

References

- [1] Knorr D B, Tracy D P. Correlation of texture with electromigration behavior in Al metallization. *Appl Phys Lett*, 1991, 59(25): 3241
- [2] Vaidya S, Sinha A K. Effect of texture and grain structure on electromigration in Al-0.5% Cu thin films. *Thin Solid Films*, 1981, 75: 253
- [3] Korhonen M A, Lafontaine W R, Børgesen P, et al. Stress-induced nucleation of void in narrow aluminum-based metallization on silicon substrates. *J Appl Phys*, 1991, 70(11): 6774
- [4] Jackson R L. Processing and integration of copper interconnects. *Solid State Technology*, 1998; 41(3): 49
- [5] Bunge H J. *Texture analysis in material science*. London: Butterworths, 1982
- [6] Zhang Jianmin, Xu Kewei. Dependence of strain-energy density on the grain orientation in FCC-polycrystalline films. *Acta Physica Sinica*, 2002, 51(11): 2562 (in Chinese) [张建民, 徐可为. 面心立方多晶薄膜中应变能密度对晶粒取向的依赖. *物理学报*, 2002, 51(11): 2562]
- [7] Riege S P, Thompson C V. Modeling of texture evolution in copper interconnects annealed in trenches. *Scripta Materialia*, 1999, 41(4): 403
- [8] Zhang Jianmin, Xu Kewei. Theory of abnormal grain growth in thin films and analysis of energy anisotropy. *Acta Physica Sinica*, 2003, 52(5): 1208 (in Chinese) [张建民, 徐可为. 薄膜中异常晶粒生长理论及能量各向异性分析. *物理学报*, 2003, 52(5): 1208]
- [9] Hau-Riege C S, Thompson C V, Marieb T N. The effects of width transitions on the reliability of interconnects. *Mater Res Soc Symp Proc*, 2000: 612
- [10] Mirpuri K, Szpunar J. Impact of annealing, surface/strain energy and line width to line spacing ratio on texture evolution in Damascene Cu interconnects. *Materials Characterization*, 2005, 54: 107
- [11] Okayabashi H, Ueno K, Saitoh S, et al. Microstructure of electroplated Cu films. *Advanced Metallization Conference Proceedings*, 1999: 93
- [12] Lee D N, Lee H J. Effect of stresses on the evolution of annealing textures in Cu and Al interconnects. *J Electron Mater*, 2003, 32(10): 1012
- [13] Zhang Xinming, Zhang Shaorui, Zhou Zhuoping, et al. Cold drawing and annealing textures of tantalum wires. *Chinese Journal of Nonferrous Metals*, 1999, 9(4): 774 (in Chinese) [张新明, 张少睿, 周卓平, 等. 钽丝的拉拔及退火织构. *中国有色金属学报*, 1999, 9(4): 774]
- [14] Randle V. Mechanism of twinning-induced grain boundary engineering in low stacking-fault energy materials. *Acta Mater*, 1999, 47(15): 4187
- [15] Randle V. Twinning-related grain boundary engineering. *Acta Mater*, 2004, 52: 4067

大马士革铜互连线织构的研究*

王晓冬^{1,†} 吉元² 钟涛兴² 李志国³ 夏洋⁴ 刘丹敏² 肖卫强²

(1 中国人民武装警察部队学院基础部, 廊坊 065000)

(2 北京工业大学固体微结构与性能研究所, 北京 100022)

(3 北京工业大学电子信息与控制工程学院, 北京 100022)

(4 中国科学院微电子中心, 北京 100029)

摘要: 采用 EBSD 研究了不同线宽和退火前后 Cu 互连线的织构和晶界特征分布. Cu 互连线均具有多重织构, 其中(111)织构强度最高. 沉积态样品在室温下发生了自退火现象, 并出现了一些异常长大的晶粒. 随高宽比降低和退火处理, Cu 互连线晶粒尺寸变大, (111)织构得到加强, 而具有较低应变程度的织构与(111)织构强度的比例下降. 沉积态样品出现了(111)〈112〉和(111)〈231〉织构组分. 退火后, 出现了(111)〈110〉组分, 而且(111)〈112〉和(111)〈231〉组分得到增强. Cu 互连线以大角度晶界为主, 其中具有 55°~60° 错配角的晶界和 $\Sigma 3$ 晶界比例最高, 35°~40° 的错配角和 $\Sigma 9$ 晶界次之. 随高宽比增加和退火处理, $\Sigma 3$ 晶界比例逐渐升高, $\Sigma 9$ 晶界比例下降.

关键词: Cu 互连线; 织构; 错配角; 重合点阵晶界; 电子背散射衍射

EEACC: 0290T

中图分类号: TN406

文献标识码: A

文章编号: 0253-4177(2008)06-1136-05

* 国家自然科学基金资助项目(批准号: 69936020)

† 通信作者. Email: wwxiaodong@yahoo.com.cn

2007-10-29 收到, 2008-02-17 定稿